DOI: 10.1002/ejic.201100567

Anion Effects in Cu-Crosslinked Palindromic Artificial Tripeptides with Pendant Bpy Ligands

Joy A. Gallagher,[a] Lauren A. Levine,[a] and Mary Elizabeth Williams*[a]

Keywords: Self-assembly / Molecular recognition / Copper / Anion effects

An artificial peptide with three pendant bipyridine (bpy) ligands on a palindromic backbone was designed and used to make multimetallic assemblies. The tripeptide is synthesized by addition of ligand-substituted aminoethylglycine monomers to both ends of a bpy-substituted diacid. The tripeptide was treated with Cu^{II} acetate, tetrafluoroborate, and nitrate salts, and the chelation stoichiometry was confirmed in spectrophotometric titrations. NMR spectroscopy, mass spectrometry, and analytical HPLC separations confirm the identity and purity of the product, which is a tripeptide duplex with three Cu^{II} coordinative crosslinks. UV/Vis absorbance and EPR spectroscopy were used to assess the geometry of the metal complexes and examine the effects of coordinative anions on the coordination geometry about the Cu centers. We find that the distorted square-planar geometry in the Cu duplex shifts to a tetrahedral geometry upon addition of I^- and that counteranions can be used to tune the interaction between metal complexes in multimetallic assemblies.

Introduction

Inorganic biomimetic structures have been designed by using biological macromolecules for inspiration.[1] Inorganic analogs have the potential for encoding tunable magnetic, electronic, chemical, and physical properties and extending these beyond the capabilities of natural systems. To create large, functional architectures, directed self-assembly is a particularly attractive and viable route. Nature employs molecular recognition of a finite number of discrete, modular units in the form of amino acids and nucleobases, which encode structure and function in a bottom-up manner for all biological process. We aim to develop structural and functional inorganic analogs of deoxyribonucleic acid (DNA), which use metals to crosslink artificial oligopeptides that assemble into multimetallic architectures for functional materials.

Our group has employed an aminoethylglycine backbone with pendant heterocyclic ligands that bind metal ions to create single-stranded,[2] duplex,[3] and hairpin[4] structures. By using solely chelating ligands, our systems assemble via metal coordinative bonds rather than hydrogen-bonding or π–π interactions of nucleic acid–base pairs. Molecular recognition between oligopeptide strands is based on metal coordinative saturation: in the presence of a tetracoordinate metal, the complementarity of artificial bases will follow a bidentate–bidentate [2 × 2] or tridentate–monodentate [3 × 1] pattern, analogous to that in adenine–thiamine [A–T] and guanine–cytosine [G–C] base pairs in DNA. Our initial work implemented solid-phase peptide synthesis to create oligopeptide strands with N and C termini.[2a,2b,3a] To eliminate the formation of parallel and antiparallel isomer duplexes and to control the alignment of the strands in metal-linked oligopeptide duplexes, we developed a synthetic strategy to prepare symmetric peptides.[5] The palindromic motif eliminates the formation of parallel and antiparallel isomers, which are possible as a result of alternating termini (Figure 1).

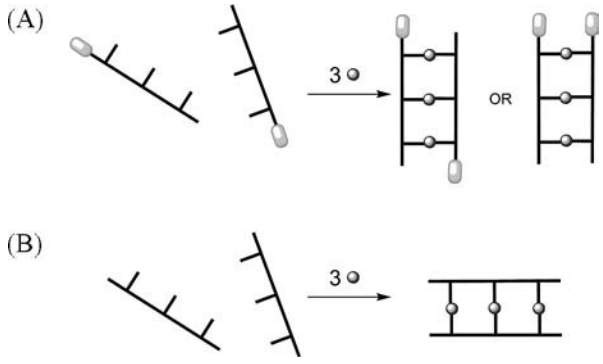

Figure 1. (A) Schematic of a metal-induced duplex formation of a monofunctional, self-complementary tripeptide with N and C termini. (B) Schematic of metal-coordination-induced parallel duplex formation with palindromic tripeptides.

In this study, the palindromic motif has been utilized to form metal-linked duplexes after the synthesis and characterization of the bpy–tripeptide. We then use these as model systems to study the role and impact of the counteranion on the geometries of the metal complex crosslinks, since this is a determining factor for the interactions between metal complexes within multimetallic assemblies.

[a] Department of Chemistry, The Pennsylvania State University, 104 Chemistry Building, University Park, PA 16802, USA
E-mail: mbw@chem.psu.edu

Supporting information for this article is available on the WWW under http://dx.doi.org/10.1002/ejic.201100567.

Results and Discussion

Synthesis and Characterization of Artificial Tripeptides

Our group has previously reported the synthesis of ligand-substituted artificial oligopeptides by solution-phase techniques, which sequentially add monomers to the growing chain terminus.[3b] In this paper, we present the synthesis and characterization of a new symmetric bipyridine tripeptide by using a strategy akin to divergent dendrimer synthesis.[6] Our initial report using the divergent synthetic strategy employed a 9-fluorenylmethoxycarbonyl (Fmoc) protecting group; however, the product and metal complexes had limited solubility.[3b] To increase solubility and overall yield, we have instead used the approach shown in Scheme 1, in which a bpy-substituted iminodiacetic acid backbone protected with ethyl esters (compound **2**) is used as the central unit. After deprotection to give terminal acid **2d**, this is reacted by using standard coupling techniques with two Fmoc-deprotected H_2N-bpy(aeg)-O*t*Bu monomers **1d** to yield tripeptide **3** in a facile one-pot synthesis. In contrast to the ligand-substituted artificial oligopeptides we have previously made,[2,3] tripeptide **3** is prepared by this route from the monomers in a single step in 54.1% yield, a significant increase in comparison with our previously reported solid-phase peptide synthesis (24.8%)[2a] and our first solution-phase tripeptide (1.19%).[3b]

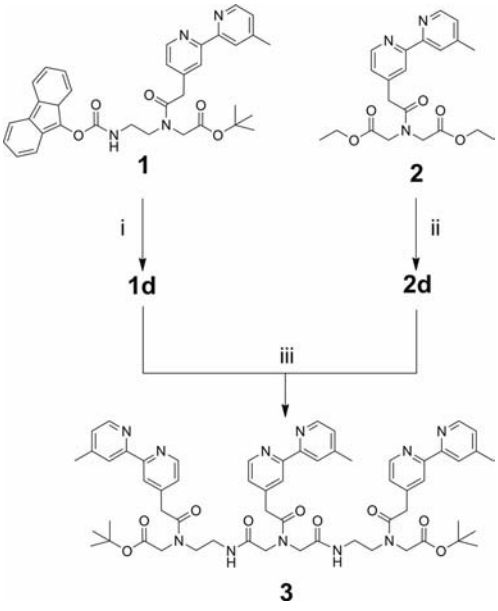

Scheme 1. Artificial tripeptide **3** synthesis. (i) 20% piperidine in ACN, 30 min; (ii) NaOH in THF overnight, 0 °C; reduce to pH to 1; (iii) 2:1 mol ratio of **1d/2d** with EDC, HOBt, DIPEA.

Synthesis and Characterization of Duplexes

Bulk-scale preparations of the Cu-containing peptide complex were performed by reacting three molar equivalents of copper(II) nitrate with two molar equivalents of the tripeptide, and the product was isolated by precipitation with sodium tetrafluoroborate or ammonium hexafluorophosphate. Alternatively, the product of the reaction with copper(II) acetate was isolated by concentration under reduced pressure, followed by recrystallization from methanol and diethyl ether. The purity was confirmed by using ^{1}H NMR spectroscopy (see Supporting Information). Although bound Cu^{2+} ions induce a paramagnetic shift of the ligand proton resonances, integration of aliphatic peaks and comparison to the amide proton peak resonances confirms that all of the tripeptide in solution has bound Cu^{2+} metal ions. HPLC was further used to assess the purity of the Cu-containing products. As we have done previously,[7] the analytical chromatograms of these complexes and of the unmetallated tripeptide were obtained by using a mobile phase of 85:15 acetonitrile with 0.1% TFA and water. The elution time of the duplexes increases with molecular weight of the counteranion: PF_6 (146 g/mol) > BF_4 (86 g/mol) > CH_3CO_2 (59 g/mol), suggesting these are tightly associated with the metallated oligopeptide structures. Vapor pressure osmometry experiments provide molecular weights that are equivalent to product species with two tripeptide strands with three bound Cu^{2+} ions, with some experimental variance that arises from residual solvent present in the Cu complexes. Together, the NMR spectra, HPLC, and vapor pressure osmometry data confirm that the predominant product of the reaction of tripeptide **3** with Cu^{2+} under these conditions is $[Cu_3\mathbf{3}_2]^{6+}$.

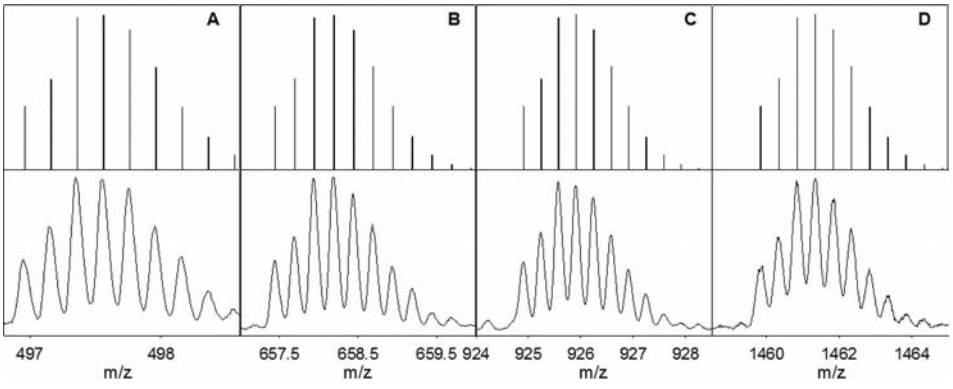

Figure 2. Molecular ion peaks observed by positive-ion electrospray mass spectrometry, plotted together with the calculated mass (above) and isotopic splitting patterns (below) for (A) $[Cu_3\mathbf{3}_2PF_6]^{5+}$, (B) $[Cu_3\mathbf{3}_2(PF_6)_2]^{4+}$, (C) $[Cu_3\mathbf{3}_2(PF_6)_3]^{3+}$, and (D) $[Cu_3\mathbf{3}_2(PF_6)_4]^{2+}$.

High-resolution electrospray mass spectrometry was used to identify the product of the reaction and compare its isotope pattern to the calculated isotope pattern. For example in Figure 2, multiple molecular ion peaks of the PF_6 salt of $[Cu_3\mathbf{3}_2]^{2+}$ are observed and correspond to species with charge +2 to +5. Rather than differences in the oxidation state of the metal ions, these molecular ions differ in charge because of the number of anions associated with the +6-charged molecular ion in the gas phase. Comparisons of these molecular ion peaks with those in theoretical spectra confirmed the identity of the species $\{[Cu_3\mathbf{3}_2](PF_6)_4\}^{2+}$, $\{[Cu_3\mathbf{3}_2](PF_6)_3\}^{3+}$, $\{[Cu_3\mathbf{3}_2](PF_6)_2\}^{4+}$, and $\{[Cu_3\mathbf{3}_2](PF_6)_1\}^{5+}$. Analogously, multiple molecular ion peaks are observed for the BF_4 salt of the $[Cu_3\mathbf{3}_2]^{6+}$ complex. However, despite exhaustive efforts we have been unable to observe molecular ion peaks for the analogous acetate complex, which may be due to differences in the charge of this complex.

Spectrophotometric Titrations

Our molecular design was based on the hypothesis that Cu^{2+} ions would form coordinative crosslinks between the pendant ligands on the tripeptides. To further investigate the stoichiometry of the reaction, the reaction of tripeptide **3** with each of the Cu^{II} salts was monitored during spectrophotometric titrations. Figure 3 contains representative difference spectra in the UV and visible regions as $Cu(BF_4)_2$ is incrementally added to a solution containing the tripeptide. In Figure 3A, addition of metal ion causes a shift in the wavelength of the peak absorbance at 670 to 722 nm, which is attributed to the d–d transition of $[Cu(bpy)_2]^{2+}$.[8] The titration curve in Figure 3B is a plot of the change in absorbance at 718 nm, which increases and levels off at a stoichiometric Cu/peptide ratio of 1.5:1 or 3:2. This stoichiometry is consistent with the molecular ions observed in the gas phase mass spectrometry experiments. At this point, the extinction coefficient of the species formed is calculated to be 100 M^{-1} cm^{-1} at 718 nm, which is consistent with the value for $[Cu(bpy)]^{2+}$. Alternatively, titration of the tripeptide with $Cu(OAc)_2$ in the Figure 3B is monitored at 920 nm and similarly contains an inflection at Cu/peptide ≈ 1.5:1. The extinction at this point is 60 M^{-1} cm^{-1} at 920 nm; the differences in extinction of the acetate and tetrafluoroborate complexes are consistent with known differences for $[Cu(bpy)_2](BF_4)_2$ at 660 nm and $[Cu(bpy)_2](OAc)_2$ at 925 nm.[8b]

In contrast to the visible absorbance spectra, four isosbestic points are observed in the UV difference spectra in Figure 3C. These are the result of a drastic redshift in the π–π* transition for the bpy ligand from 278 to 302 nm

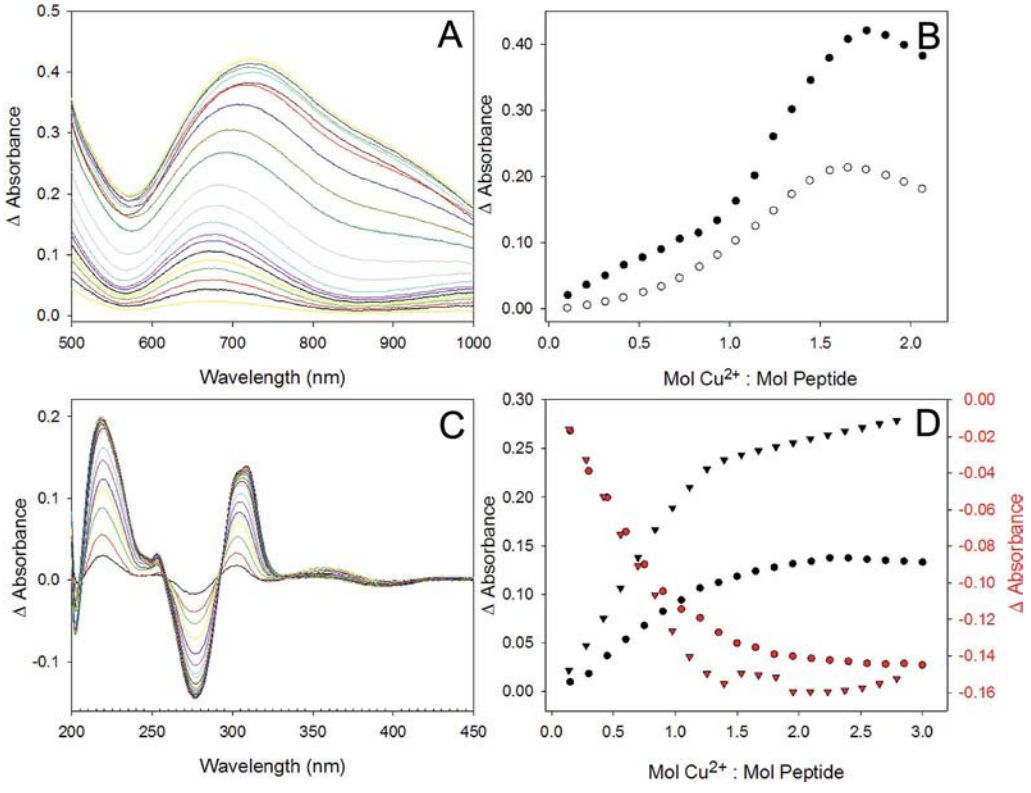

Figure 3. Spectrophotometric titration of the reaction of Cu^{2+} with the tripeptide in spectroscopic grade methanol: (A) 15 mM $Cu(BF_4)_2$ titrated in 50 μL increments into 3.16 mM tripeptide **3**. (B) Plot of the change in the absorbance at 712 nm vs. molar ratio of added Cu^{2+} to peptide for $Cu(BF_4)_2$ titration monitored at 718 nm (full circles) and $Cu(OAc)_2$ titration monitored at 920 nm (empty circles). (C) Difference spectra acquired during the spectrophotometric titration of the reaction of Cu^{2+} with 2.5 mL of 14.5 μL tripeptide **3** in methanol. Cu^{2+} is added in 50 μL increments of 100 μM $Cu(BF_4)_2$. (D) Plots of the change in the absorbance as a function of the relative molar ratio of added Cu^{2+} to **3**; $Cu(BF_4)_2$ titration monitored at 310 nm (black circles) and 277 nm (red circles); $Cu(OAc)_2$ titration monitored at 310 nm (black triangles) and 277 nm (red triangles).

upon metal ion binding[9] as well as a slight increase followed by a decrease in intensity of the peak at 357 and 394 nm, which we hypothesize is due to charge transfer between the bipyridine ligands.[10] Titration curves (Figure 3D) at 274 and 310 nm each contain a stoichiometric point at a Cu^{+2}/tripeptide mol ratio of 1.5:1, again consistent with the formation of a trimetallic species with three $[Cu(bpy)_2]^{2+}$ complexes forming crosslinks between two tripeptide strands, similar to the titration curve at 712 nm. Spectrophotometric titration data of $Cu(NO_3)_2$ and $Cu(CH_3CO_2)_2$ are found in the Supporting Information. At the equivalence point, the extinction coefficients at 310 nm are approximately 17,000 and 11,000 M^{-1} cm^{-1} for the OAc and BF_4 titrations, respectively, which compare favorably with the values measured for both the duplex structures and literature reports for $[Cu(bpy)]^{2+}$ at 310 nm.[9a]

Role of the Counteranion

The coordination geometry of $[Cu(bpy)_2]^{2+}$ has been shown to be impacted by the counteranions.[8,11] For example, $[Cu(bpy)_2](BF_4)_2$ is known to have either a distorted tetrahedral geometry, where the BF_4 does not interact with the Cu center,[11] or an elongated rhombic octahedral one, in which the BF_4^- anions are loosely coordinated in the axial position.[8,12] The $[Cu(bpy)_2NO_3]^+$ stereochemistry has been classified as *cis*-distorted octahedral,[13] and $[Cu(bpy)_2]I_2$ is known to adopt a distorted trigonal bipyramidal geometry.[14] Although it is known that anion effects alone cannot dictate the geometry around the Cu center[15] and that steric effects can play a strong role, it is clear from the anion-dependent geometries of these small molecule analogs that this may have an impact in our trimetallic structures. We therefore investigated the role of the counterion on the Cu coordination geometry by monitoring changes in the electronic absorbance spectra at the d–d Cu transition and the electron paramagnetic resonance (EPR) spectra, since these could be used to tune structure and electronic communication in the Cu-linked tripeptide duplexes.

To rapidly assay for impacts of the anion on the visible absorbance in this region, titrations with a series of sodium salts (I^-, Br^-, Cl^-, NO_3^-, $CH_3CO_2^-$, and BF_4^-) were performed in a 96-well plate and measured by using a microplate reader. Spectral changes of the d–d transition of the Cu^{II} centers for the $[Cu_3\mathbf{3}_2]^{6+}$ are compared to what is known for the small molecule $[Cu(bpy)_2]^{2+}$ analogs; for example, changes in absorbance at 770 nm were chosen for both BF_4 and OAc salts of the Cu complex, because of the significant spectral increase and slight redshift in the λ_{max} at the d–d transition region upon addition of NaI. Figure 4 compares the change in absorbance per molar equivalent of added salt for each of the series of sodium salts. These data reveal that the most extensive spectral shifts occur upon addition of NaI, which causes increased extinction and a redshift of the peak absorbance for both the OAc and BF_4 complexes. This increase in absorbance levels off at a NaI/$[Cu_3\mathbf{3}_2]^{6+}$ ratio of approximately 6:1, suggesting that six I^- anions associate to the duplex, presumably in the Cu^{II} axial positions by displacement of more weakly associated anions, thereby affecting the coordination environment. Increased extinction in the electronic absorbance spectra further suggests a distortion of the square-planar coordination geometry. Table 1 summarizes the spectral changes caused by the addition of salt to each Cu tripeptide complex. The degree of spectral shifts and changes in extinction are indicative of the affinity for the Cu complexes and changes in the molecular geometry.

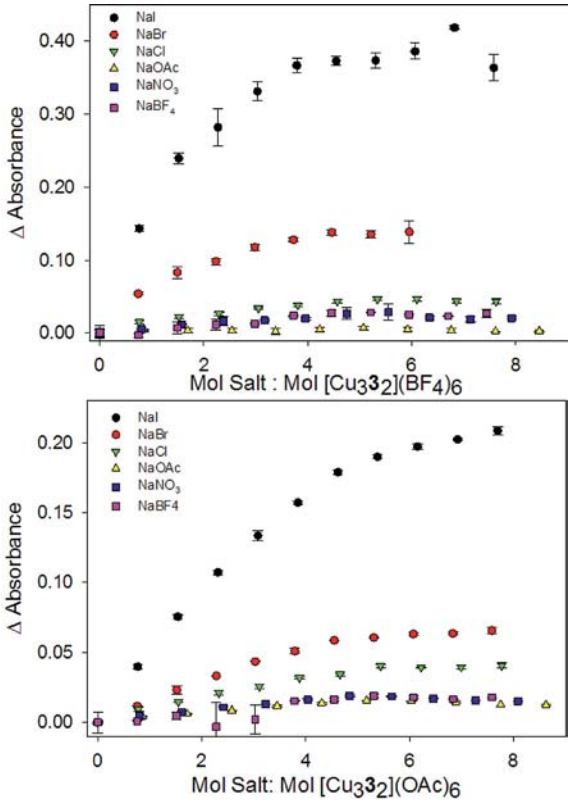

Figure 4. Change in absorbance of solutions containing (top) 0.53 M $[Cu_3\mathbf{3}_2](BF_4)_6$ or (bottom) 0.52 M $[Cu_3\mathbf{3}_2](OAc)_6$ duplexes as a function of increasing mol of salt, as indicated, in spectroscopic grade methanol.

Table 1. Absorbance data for salt titrated into $[Cu_3\mathbf{3}_2](BF_4)_6$ and $[Cu_3\mathbf{3}_2](OAc)_6$ recorded in air at room temperature in spectroscopic grade MeOH.

Salt added	$[Cu_3\mathbf{3}_2](BF_4)_6$ λ_{max} (nm)[a]	ε (M^{-1} cm^{-1})[b]	$[Cu_3\mathbf{3}_2](OAc)_6$ λ_{max} (nm)[a]	$\Delta\varepsilon$ (M^{-1} cm^{-1})[b]
	715		680	
NaI	770	259	761	101
NaBr	745	76	741	48
NaCl	738	45	710	35
NaOAc	703	14	680	24
$NaNO_3$	715	27	680	25
$NaBF_4$	715	30	680	25

[a] Peak absorbance after addition of six molar equivalents of salt to complex. [b] Change in extinction at λ_{max}.

Redshift and intensity enhancement of the d–d bands are recognized indicators of the transformation from square-planar to tetrahedral stereochemistry, since the symmetry

of the ligand field is decreased allowing for easier d–d transitions as electric dipole transitions.[16] The electronic absorption spectral changes predict that the intensity of a d–d transition will increase as the symmetry of the ligand field decreases. Since the d–d transitions become allowed as electric dipole transitions, I^- has the largest spectral impact followed by Br^-. Whereas addition of OAc^- to the $[Cu_3\mathbf{3}_2](BF_4)_6$ complex induces spectral shifts, the opposite is not true. Using the data in Figure 4 and Table 2, we can compare the degree of spectral shift and change in absorbance; it appears that the trend in the extent of anion association with the trimetallic duplex is: $I^- > Br^- > CH_3CO_2^- > Cl^- \approx NO_3^- \approx BF_4^-$.

Table 2. Measured ***g*** tensor and hyperfine coupling constants from EPR spectra.

Complex	$g_\parallel$	$g_\perp$	$A_\parallel$ (10^{-4} cm^{-1})
$[Cu_3\mathbf{3}_2](BF_4)_6$	2.183	2.098	161
$[Cu_3\mathbf{3}_2](BF_4)_6$ + 6NaI	2.198	2.094	182
$[Cu_3\mathbf{3}_2](OAc)_6$	2.228	2.124	
$[Cu_3\mathbf{3}_2](OAc)_6$ + 6NaI	2.203	2.107	

The observed influences of the counterion in the absorbance spectra led us to characterize the molecular geometries with use of EPR spectroscopy. Figure 5 contains the EPR spectra of solutions containing $[Cu_3\mathbf{3}_2](BF_4)_6$ and $[Cu_3\mathbf{3}_2](OAc)_6$; analysis of these provides the ***g*** tensor values and hyperfine couplings listed in Table 2. The tensor values in the range $g_\parallel > 2.1 > g_\perp > 2.0$ and hyperfine coupling constant $A_\parallel > 130$ (cm^{-1}/ 10^{-4}) suggest that the Cu^{II} geometry is tetragonal.[17] The $g_\parallel/A_\parallel$ quotient value of 135 cm for $[Cu_3\mathbf{3}_2](BF_4)_6$ is at the upper limit of the range assigned to square-planar geometry, suggesting a distortion toward tetrahedral geometry.[18] Values of the ***g*** tensor for $[Cu_3\mathbf{3}_2](OAc)_6$ are also in the range $g_\parallel > 2.1 > g_\perp > 2.0$, suggesting a tetragonal coordination sphere; however, the lack of hyperfine interaction for the $[Cu_3\mathbf{3}_2](OAc)_6$ duplex indicates that the metal centers are at a distance greater than 6 Å.[19] At this distance, it is unlikely that acetate bridges two Cu centers.[20]

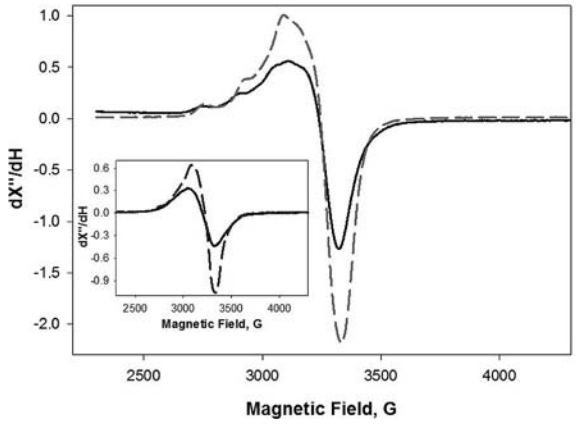

Figure 5. EPR spectra of 0.53 mM $[Cu_3\mathbf{3}_2](BF_4)_6$ (solid line) along with the same solution containing 6 molar equivalents of NaI (dashed line). The inset contains the EPR spectra of 0.52 mM $[Cu_3\mathbf{3}_2](OAc)_6$ (solid line) in methanol together with this solution containing 6 molar equivalents of NaI (dashed line).

Since the addition of NaI caused the most dramatic changes in the electronic absorbance spectra, we examined the EPR spectra of the complexes with six molar equivalents of added NaI. In Figure 5 (dashed lines), added NaI results in increases in $g_\parallel$, $g_\perp$, and $A_\parallel$. The $g_\parallel/A_\parallel$ value (120 cm) for $[Cu_3\mathbf{3}_2](BF_4)_6$ with NaI suggests that the soft anion I^- associates with Cu in the axial positions. The lack of hyperfine interactions for $[Cu_3\mathbf{3}_2](OAc)_6$ with NaI suggests that the addition of I^- prevents nuclear interactions of the Cu centers and deforms these toward distorted-tetrahedral geometry.[21] Insertion of anions in the trimetallic structure and distortion of geometry is likely to cause an increase in the metal–metal distances. Because the aeg backbone is flexible, the tripeptide is able to accommodate the I^- anions. However, the dynamic motions of the molecule have also made crystallographic-quality crystals elusive, so that in our ongoing efforts we use the high-energy beam of the synchrotron to determine the metal–metal distances in solution.

Conclusions

Using the symmetric bipyridine tripeptide as a platform, we have investigated the formation of $[Cu(bpy)_2]^{2+}$ crosslinked tripeptide duplexes and the role of the counteranion on the resulting trimetallic structure. We find that association with anions in the axial positions has observable impact on the absorbance and EPR spectra, which is indicative of impacts on the complex geometry. Because coupling between adjacent metal ions is important for electron transfers in the structures and for long-range photoinduced charge separation in chromophore-linked assemblies and molecular materials,[4a,4c] these studies reveal the important and felxible role that axial ligation can play in tuning the functionality of multimetallic structures.

Experimental Section

Instrumentation and Analysis: UV/Vis absorbance spectra were obtained with a double-beam spectrophotometer (Varian, Cary 500) by using a 1-cm quartz cuvette. The salt titrations were performed with a Molecular Devices SpectraMax M2 microplate reader. Mass spectrometric analysis was performed with a Waters LCT Premier time-of-flight (TOF) mass spectrometer. Samples were introduced into the mass spectrometer by using direct infusion via a syringe pump built into the instrument. The mass spectrometer was set to scan the range m/z = 100–2500 in the positive-ion mode, with electrospray ionization (ESI). The drying gas temperature was set to 80 °C, and the capillary voltage was 2200 V. X-band electron paramagnetic resonance (EPR) spectra were acquired with a 9.5 GHz Bruker ESP-300 spectrometer with a liquid He cryostat at 12.9 K with 5 mW power and 10.2 G modulation amplitude. ^{1}H, ^{13}C, HMQC, HMBC, and COSY NMR spectra were collected with a 400 MHz spectrophotometer (Bruker).

Chemicals: The syntheses of 4′-methyl-2,2′-bipyridine-4-acetic acid,[22] *tert*-butyl *N*-[2-(*N*-9-fluorenylmethoxycarbonyl)amino-

ethyl]glycinate hydrochloride (Fmoc-aeg-O*t*Bu·HCl),[23] and *tert*-butyl {*N*-[2-(*N*-9-fluorenylmethyoxycarbonylamino)ethyl]-*N*-[2-(4′-methyl-2,2′-bipyridyl)acetyl]amino}acetate [Fmoc-aeg(Bpy)-O*t*Bu][4b] (**1**) were performed as reported. *N*-hydroxybenzotriazole (HOBT) and 1-ethyl-3-(3-dimethylaminopropyl)carbodiimide hydrochloride (EDC) were purchased from Advanced ChemTech. *O*-Benzotriazole-*N*,*N*,*N*′,*N*′-tetramethyluronium hexafluorophosphate (HBTU) was purchased from NovaBiochem. All solvents were used as received without further purification unless otherwise noted.

Syntheses

Diethyl Iminodiacetate: By using a modified literature method,[24] iminodiacetic acid (10.33 g, 77.7 mmol) was added to hydrochloric acid (100 mL of 2.5 M in ethanol). This solution was heated at reflux for 24 h and then allowed to cool to room temperature. Water (ca. 200 mL) was added, and the solution was neutralized with sodium hydrogen carbonate. The solution was extracted with dichloromethane (3 × 75 mL), and the combined organic solutions were dried with sodium sulfate. The solvent was removed under vacuum to yield 3.62 g of colorless oil (38.4%). MS (ESI$^+$): calcd. for [M + H]$^+$ 190.1; found 190.3. ^{1}H NMR (400 MHz, $CDCl_3$): δ = 1.13 (t, J = 7 Hz, 6 H), 2.10 (s, 1 H), 3.35 (s, 4 H), 4.10 (q, J = 7 Hz, 4 H) ppm.

Ethyl [*N*-2-(4′-Methyl-2,2′-bipyridyl)acetyl]iminodiacetate (EtO-Bpy-OEt) (2): 4′-methyl-2,2′-bipyridine-4-acetic acid (3.40 g, 14.0 mmol), HBTU (5.29 g, 14.0 mmol), and HOBT (1.89 g, 14.0 mmol) were added to dry dichloromethane (150 mL) stirred in an ice bath. The suspension was stirred for 15 min, DIPEA (4.6 mL, 27.9 mmol) was added, and the yellow solution was stirred for an additional 45 min. To this was added diethyl iminodiacetate (1.32 g, 7.0 mmol) in dry dichloromethane (50 mL), and the solution was allowed to reach room temperature. After stirring for 24 h, the solvent was removed under vacuum, and the product was isolated and purified by silica column chromatography with a mobile phase of methanol (5%) in dichloromethane. Like fractions were combined, and the solvent was evaporated to yield 1.29 g of yellow oil (46.3%). MS (ESI$^+$): calcd. for [M + H]$^+$ 400.4; found 400.5. ^{1}H NMR (400 MHz, $CDCl_3$): δ = 1.2 (m, 6 H), 2.10 (s, 1 H), 2.40 (s, 3 H), 3.45 (s, 4 H), 3.7–3.8 (s, 2 H), 4.15 (m, 4 H), 8.60–7.18 (d, J = 64 Hz, 2 H), 7.89–8.16 (d, J = 36 Hz, 2 H), 8.3–8.5 (d, J = 41 Hz, 2 H) ppm.

Ethyl [*N*-2-(4′-Methyl-2,2′-bipyridyl)acetyl]iminodiacetic Acid (2d): According to an adapted synthesis,[25] compound **2** (1.29 g, 3.2 mmol) was dissolved in tetrahydrofuran (13 mL), and sodium hydroxide (8 mL, 2 M) was added dropwise and allowed to stir overnight. Water (25 mL) was added and extracted with dichloromethane (2 × 50 mL). The aqueous layer was retained and cooled by stirring over ice. The pH was lowered to 7 with HCl (2 M), and the solvent was removed under vacuum to yield 1.05 g of bright yellow solid (94.7%). MS (ESI$^+$): calcd. for [M + H]$^+$ 344.3; found 344.2. ^{1}H NMR (400 MHz, MeOD): δ = 2.50 (s, 3 H), 3.27 (s, 4 H), 3.86 (s, 2 H), 7.19–7.47 (dd, J = 4, 69 Hz, 2 H), 7.92–8.26 (d, J = 43 Hz, 2 H), 8.3–8.75 (dd, J = 25, 5 Hz, 2 H) ppm.

***tert*-Butyl {*N*-[2-Aminoethyl]-*N*-[2-(4′-methyl-2,2′-bipyridyl)-acetyl]-amino} Acetate (1d):** This synthesis was adapted from a published procedure.[26] To **1** (2.64 g, 4.4 mmol) was added dropwise piperidine (140 mL, 20%) in acetonitrile. The solution was stirred for 30 min and extracted with hexanes (3 × 75 mL). The acetonitrile layer was reduced under vacuum to yield 1.65 g of yellow oil (98.6%). MS (ESI$^+$): calcd. for [M + H]$^+$ 385.5; found 385.2. ^{1}H NMR (400 MHz, $CDCl_3$): δ = 1.33 (s, 9 H), 2.33 (s, 3 H), 2.70 (t, J = 5 Hz, 2 H), 3.10–3.35 (q, J = 8 Hz, 2 H), 3.60 (m, 2 H), 6.85 (t, J = 5 Hz, 1 H), 7.0–7.22 (dd, J = 5, 61 Hz, 2 H), 8.04–8.19 (d, J = 34 Hz, 2 H), 8.36–8.52 (dd, J = 5, 35 Hz, 2 H) ppm.

***tert*-Butyl-(aeg)(bpy)-(diamide)(bpy)-(aeg)(bpy)-*tert*-butyl (3):** In an ice bath, **2d** (0.50 g, 1.5 mmol), EDC (0.70 g, 3.7 mmol), and HOBt (0.50 g, 3.7 mmol) were added to dry dichloromethane (75 mL). The suspension was stirred for 15 min and DIPEA (1.5 mL, 8.9 mmol) was added. The yellow solution was allowed to stir for an additional 90 min and **1d** (2.2 g, 5.7 mmol) was added. The solution was allowed to react for four days, and the volume was then reduced under vacuum. The product was purified by column chromatography using a 10% methanol/90% dichloromethane mobile phase. Like fractions were combined to yield 0.85 g of yellow foam (54.1%). HRMS (ESI$^+$): calcd. for [M + H]$^+$ 1076.5358; found 1076.5358. $C_{59}H_{69}N_{11}O_9{\cdot}CH_3OH{\cdot}CH_2Cl_2$: calcd. C 61.69, H 6.39, N 12.93; found C 61.43, H 6.36, N 12.92. See Supporting Information for ^{1}H and ^{13}C NMR spectral assignments.

$Cu_3[3]_2(BF_4)_6$ and $Cu_3[3]_2(PF_6)_6$: In a 50 mL round-bottomed flask, **3** (141 mg, 0.13 mmol) and copper(II) nitrate hexahydrate (45.9 mg, 0.19 mmol) were added to methanol (ca. 10 mL) and heated at reflux overnight. To produce the BF_4 salt, the solution was cooled to room temperature, and the solvent was evaporated under vacuum. The remaining mixture was redissolved in a 1:4 mixture of methanol/water, and a saturated aqueous solution of ammonium tetrafluoroborohyrate was slowly added. The product was filtered and washed with methanol and diethyl ether. The olive-green powder was dried under vacuum overnight to yield 75.6 mg (20.1%). ^{1}H NMR (400 MHz, [D$_3$]ACN, Figure S5): δ = 4.67–2.57 (br. m, 44 H), 1.57–1.23 (br. s, 36 H) ppm. MS (ESI$^+$): calcd. for $\{[Cu_3(\mathbf{3})_2](BF_4)_2\}^{+4}$ 628.9; found 631.0; calcd. for $\{[Cu_3(\mathbf{3})_2](BF_4)_4{\cdot}CH_3CN\}^{+2}$ 1357.9; found 1359.4. To produce the PF_6 salt, a saturated solution of hexafluorophosphate was added to precipitate the copper duplex, and the product was isolated and purified as before. For $[Cu_3(\mathbf{3})_2](PF_6)_x$: MS (ESI$^+$) (Figure 3): calcd. for $\{[Cu_3(\mathbf{3})_2](PF_6)_4\}^{+2}$ 1461.4; found 1461.2; calcd. for $\{[Cu_3(\mathbf{3})_2](PF_6)_3\}^{+3}$ 925.9; found 925.6; calcd. for $\{[Cu_3(\mathbf{3})_2](PF_6)_2\}^{+4}$ 658.2; found 658.2; calcd. for $\{[Cu_3(\mathbf{3})_2](PF_6)\}^{+5}$ 497.6; found 497.6. ^{1}H NMR (400 MHz, [D$_3$]ACN, Figure S7): δ = 4.74–2.43 (br. m, 44 H), 1.54–1.31 (br. s, 36 H) ppm.

$Cu_3[3]_2(CH_3CO_2)_6$: In a 50 mL round-bottomed flask, compound **3** (126 mg, 0.117 mmol) and copper acetate (34.3 mg, 0.176 mmol) were stirred in methanol overnight. The solution was recrystallized from methanol and diethyl ether, washed with H_2O, collected, and dried overnight to yield an emerald green powder, yield 151 mg (47.8%). ^{1}H NMR (400 MHz, [D$_3$]ACN, Figure S6): δ = 4.74–2.43 (br. m, 44 H), 1.54–1.31 (br. s, 36 H) ppm.

Spectrophotometric Titrations: Titrations were performed by using spectroscopic grade methanol solutions of known concentrations of tripeptide and $Cu(NO_3)_2$, $Cu(BF_4)_2$, and $Cu(CH_3COO)_2$. For measurements of visible wavelength absorbance, approximately 15 mM Cu^{2+} was titrated into approximately 3 mM tripeptide; and for absorbance measurements in the ultraviolet region, approximately 100 μM Cu^{2+} was titrated into approximately 15 μM tripeptide solution. Background subtractions were performed by using the double beam of the spectrometer.

Spectrophotometric Titrations with Addition of Salts: Titrations were performed by using spectroscopic grade methanol solutions of approximately 0.5 mM Cu^{2+} duplexes (BF_4 and CH_3CO_2), to which approximately 10 mM salts (NaI, NaBr, NaCl, $NaNO_3$, $NaCH_3CO_2$, and $NaBF_4$) were added incrementally, and the process was monitored with a BD Falcon 96 well-plate and well-plate reader in the visible region.

Supporting Information (see footnote on the first page of this article): NMR spectroscopic data, spectrophotometric titrations of $Cu(NO_3)_2$ and $Cu(CH_3O_2)_2$ into **3**.

Acknowledgments

We gratefully acknowledge support from the Chemical Sciences, Geosciences, and Biosciences Division of the Office of Basic Energy Sciences of the U. S. Department of Energy (DE-FG02-08ER15986). We thank James Miller in the Mass Spectrometry Facility, Professor S. Booker and T. Grove for their assistance with the EPR spectra, and Professor D. Boehr for the use of the microplate reader.

[1] a) L. A. Levine, M. E. Williams, *Curr. Opin. Chem. Biol.* **2009**, *13*, 669–677; b) M. Sarikaya, C. Tamerler, A. K. Y. Jen, K. Schulten, F. Baneyx, *Nat. Mater.* **2003**, *2*, 557–585; c) D. Gust, T. A. Moore, A. L. Moore, *Acc. Chem. Res.* **2009**, *42*, 1890–1898; d) A. Magnuson, M. Anderlund, O. Johansson, P. Lindblad, R. Lomoth, T. Polivka, S. Ott, K. Stensjo, S. Styring, V. Sundstrom, L. Hammarstrom, *Acc. Chem. Res.* **2009**, *42*, 1899–1909.

[2] a) B. P. Gilmartin, K. Ohr, R. L. McLaughlin, R. Koerner, M. E. Williams, *J. Am. Chem. Soc.* **2005**, *127*, 9546–9555; b) K. Ohr, B. P. Gilmartin, M. E. Williams, *Inorg. Chem.* **2005**, *44*, 7876–7885; c) L. A. Levine, H. W. Youm, H. P. Yennawar, M. E. Williams, *Eur. J. Inorg. Chem.* **2008**, *26*, 4083–4091.

[3] a) K. Ohr, R. L. McLaughlin, M. E. Williams, *Inorg. Chem.* **2007**, *46*, 965–974; b) B. P. Gilmartin, R. L. McLaughlin, M. E. Williams, *Chem. Mater.* **2005**, *17*, 5446–5454.

[4] a) C. P. Myers, J. R. Miller, M. E. Williams, *J. Am. Chem. Soc.* **2009**, *131*, 15291–15300; b) L. A. Levine, S. I. Kirin, C. P. Myers, S. A. Showalter, M. E. Williams, *Eur. J. Inorg. Chem.* **2009**, *5*, 613–621; c) C. P. Myers, B. P. Gilmartin, M. E. Williams, *Inorg. Chem.* **2008**, *47*, 6738–6747.

[5] a) F. Zeng, S. C. Zimmerman, *Chem. Rev.* **1997**, *97*, 1681–1712; b) Y. Haba, A. Harada, T. Takagishi, K. Kono, *J. Am. Chem. Soc.* **2004**, *126*, 12760–12761; c) S. Mattei, P. Seiler, F. Diederich, V. Gramlich, *Helv. Chim. Acta* **1995**, *78*, 1904–1912; d) G. R. Newkome, X. Lin, *Macromolecules* **1991**, *24*, 1443–1444; e) L. Crespo, G. Sanclimens, M. Pons, E. Giralt, M. Royo, F. Albericio, *Chem. Rev.* **2005**, *105*, 1663–1681.

[6] a) D. A. Tomalia, H. Baker, J. Dewald, M. Hall, G. Kallos, J. R. Martin, J. Ryder, P. Smith, *Polym. J.* **1985**, *17*, 117–132; b) G. R. Newkome, V. K. Gupta, G. R. Baker, Z. Q. Yao, *J. Org. Chem.* **1985**, *50*, 2003–2004; c) C. J. Hawker, J. M. J. Fréchet, *J. Am. Chem. Soc.* **1990**, *112*, 7638–7647; d) C. J. Hawker, J. M. J. Fréchet, *J. Chem. Soc., Chem. Commun.* **1990**, *15*, 1010–1011.

[7] a) M. B. Coppock, J. R. Miller, M. E. Williams, *Inorg. Chem.* **2011**, *50*, 949–955; b) M. B. Coppock, M. T. Kapelewski, H. W. Youm, L. A. Levine, J. R. Miller, C. P. Myers, M. E. Williams, *Inorg. Chem.* **2010**, *49*, 5126–5133.

[8] a) J. Foley, S. Tyagi, B. J. Hathaway, *J. Chem. Soc., Dalton Trans.* **1984**, *1*, 1–5; b) B. J. Hathaway, I. M. Procter, R. C. Slade, A. A. G. Tomlinson, *J. Chem. Soc. A* **1969**, 2219–2224.

[9] a) K. Stone, P. Krumholz, H. Stammreich, *J. Am. Chem. Soc.* **1955**, *77*, 777–780; b) S. F. Lincoln, F. Aprile, H. W. Dodger, J. P. Hunt, *Inorg. Chem.* **1965**, *4*, 929–935.

[10] P. S. Subramanian, E. Suresh, P. Dastidar, S. Waghmode, D. Srinivas, *Inorg. Chem.* **2001**, *40*, 4291–4301.

[11] C. Biswas, M. B. G. Drew, M. Estrader, A. Ghosh, *J. Chem. Soc., Dalton Trans.* **1981**, *2*, 567–574.

[12] a) J. Foley, D. Kennefick, D. Phelan, S. Tyagi, B. J. Hathaway, *J. Chem. Soc., Dalton Trans.* **1983**, *10*, 2333–2338; b) R. M. Williams, L. De Cola, F. Hart, J. J. Lagref, J. M. Planeix, A. De Cian, M. W. Hosseini, *Coord. Chem. Rev.* **2002**, *230*, 253–261.

[13] C. J. Simmons, A. Clearfield, W. Fitzgerald, S. Tyagi, B. J. Hathaway, *Inorg. Chem.* **1983**, *22*, 2463–2466.

[14] H. Elliot, B. J. Hathaway, R. C. Slade, *J. Chem. Soc. A* **1966**, 1443–1445.

[15] a) E. Prenesti, P. G. Daniele, S. Berto, S. Toso, *Polyhedron* **2006**, *25*, 2815–2823; b) G. A. van Albada, A. Mohamadou, I. Mutikainen, U. Turpeinen, J. Reedijk, *Eur. J. Inorg. Chem.* **2004**, 3733–3742.

[16] H. Yokoi, A. W. Addison, *Inorg. Chem.* **1977**, *16*, 1341–1348.

[17] a) N. Wei, N. N. Murthy, K. D. Karlin, *Inorg. Chem.* **1994**, *33*, 6093–6100; b) T. Vanngard in *Biological Applications of Electron Spin Resonance*, Wiley-Interscience, New York, **1972**, p. 411–447.

[18] a) U. Sakaguchi, A. W. Addison, *J. Chem. Soc., Dalton Trans.* **1979**, *4*, 600–608; b) J. A. Hartman, A. L. Kammier, R. J. Spracklin, W. H. Pearson, M. Y. Combariza, R. W. Vachet, *Inorg. Chim. Acta* **2004**, *357*, 1141–1151; c) H. Yokoi, A. W. Addison, *Inorg. Chem.* **1977**, *16*, 1341–1348.

[19] E. I. Solomon, U. M. Sundaram, T. E. Machonkin, *Chem. Rev.* **1996**, *96*, 2563–2605.

[20] R. J. Doedens, S. J. Lippard, "Structure, Metal–Metal Interactions in Copper(II) Carboxylate Complexes" in *Progress in Inorganic Chemistry: Vol. 21*, John Wiley & Sons, Hoboken, NJ, **1976**.

[21] B. J. Hathaway, *Struct. Bonding (Berlin)* **1984**, *57*, 55–118.

[22] L. Della Ciana, I. Hamachi, T. J. Myer, *J. Org. Chem.* **1989**, *54*, 1731–1735.

[23] S. A. Thomason, J. A. Josey, R. Cadilla, M. D. Gual, C. F. Hassman, M. J. Luzzio, A. J. Piper, K. L. Reed, D. J. Ricca, R. W. Wieth, S. A. Noble, *Tetrahedron* **1995**, *51*, 6179–6194.

[24] N. Valls, V. M. Segarra, X. Lopez, J. Bosch, *Heterocycles* **1989**, *29*, 231–235.

[25] K. L. Dueholm, M. Egholm, C. Behrens, L. Christensen, H. F. Hansen, T. Vulpius, K. H. Petersen, P. E. Nielsen, O. Buchardt, *J. Org. Chem.* **1994**, *59*, 5767–5773.

[26] B. Nawrot, B. Rebowska, K. Cieslinska, W. J. Stec, *Tetrahedron Lett.* **2005**, *46*, 6641–6644.

Received: June 4, 2011
Published Online: August 2, 2011

